Revisit two short-range interacting particles trapped in a harmonic potential

Xilin Zhang*
Department of Physics, The Ohio State University, Columbus, Ohio 43210, USA and
Physics Department, University of Washington, Seattle, WA 98195, USA
(Dated: April 18, 2019)

In this work, I revisit a non-relativistic problem concerning the dynamics of two short-range interacting particles in a background field/potential trap taking the form of harmonic potential. It was suggested their free-space scattering phase shifts can be extracted from their energy spectra with the trap turned on, but the existing formula for this purpose is exact only for infinitely shallow trap. The current study provides a systematical improvement over the formula so that deeper traps can be implemented. This paves the way for extracting nuclear scattering phase-shift from *ab initio* nuclear many-body structure calculations, a long-sorted goal in nuclear physics, and also establishes effective field theory as a useful framework to study the connection between structure information of a trapped system (with two or even more sub-clusters) and continuum physics including reactions.

Introduction— In 1998 and the field of cold atom physics, T. Busch *et.al.,* derived an interesting formula [1] stating that the energy spectra of two non-relativistic short-range interacting particles confined in harmonic potential traps are directly related to the their free-space scattering phase shifts at those eigen-energies. The following studies in condensed matter focus on improving the original formula in various directions [2–5]. In Refs. [5, 6], the formula for general angular momentum l (named as BERW formula from now on) is

$$p^{2l+1}\cot\delta_l(E) = (-)^{l+1}(4M_{\rm R}\omega)^{l+\frac{1}{2}}\frac{\Gamma\left(\frac{3}{4}+\frac{l}{2}-\frac{E}{2\omega}\right)}{\Gamma\left(\frac{1}{4}-\frac{l}{2}-\frac{E}{2\omega}\right)} \quad (1)$$

Here, $E \equiv p^2/(2M_{\rm R})$ being the eigen-energies of the system—with the center of mass (CM) energy subtracted—in a trap whose potential is $\omega^2\boldsymbol{r}^2/2$ times the mass of individual particle; $M_{\rm R}$ is the effective mass for the relative dynamics; δ_l is the corresponding phase shift. Such connection bares great similarity to the one born out of Luscher formula [7] which is widely used in the field of Lattice Quantum ChromoDynamcs for extracting two-particle scattering information from their spectra in a space-time volume with periodic boundary condition. Not surprisingly the related studies in nuclear physics [6, 8–10] were testing whether the BERW formula could be used to compute nuclear scattering from *ab initio* nuclear many-body spectra calculations.

Unfortunately, the BERW formula is only exact at $\omega \to 0$ limit, because the external potential modifies two particles' interaction at short distance. Even worse the modification increases with ω. To illustrate the issue's impact on the phase-shift extraction, I use a two-body square potential well model [11] designed for describing neutron-α nucleus scatterings as a test bed. Fig. 1 shows the p-wave ($3/2^-$ channel for neutron-α) phase shifts extracted using Eq.(1) at the trapped system's eigen-energies ($\omega = 2, 4, 6$ MeV): the extractions are in clear disagreement [6] and systematically deviate from the exact phase-shift curve (labeled as the "True" curve).

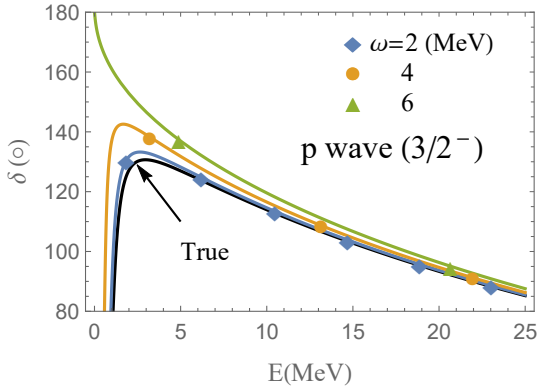

FIG. 1. Illustration. understand the formula's failure, new formula, and how nuclear physics uses it

This issue hasn't been systematically and satisfactorily addressed until the current work. Here, the pionless effective field theory (EFT) framework [12–14] is used, which is suitable for studying low-energy finite-range-interaction dynamics without resorting to a particular parameterization of the underlying potential. It has also been used to re-derive and generalize the Luscher formula [15, 16]. The improved BERW formula is

$$\sum_{\substack{i=0\\j=0}}^{\infty} C_{i,j}\frac{b^{-4i}p^{2j}}{M_H^{4i+2j}} = (-)^{l+1}\left(\frac{2b^{-1}}{M_H}\right)^{2l+1}\frac{\Gamma\left(\frac{3}{4}+\frac{l}{2}-\frac{E}{2\omega}\right)}{\Gamma\left(\frac{1}{4}-\frac{l}{2}-\frac{E}{2\omega}\right)}, \quad (2)$$

$$\left(\frac{p^2}{M_H^2}\right)^{l+\frac{1}{2}}\cot\delta_l(E) = \sum_{j=0}^{\infty} C_{i=0,j}\left(\frac{p^2}{M_H^2}\right)^j. \quad (3)$$

I have introduced a reference scale M_H with proper powers to make parameters dimensionless, and invoked the effective range expansion (ERE) [12, 14] in Eq.(3) for the phase-shifts. The formula suggests for a trap with given ω, the "phase-shift" extracted using Eq.(1) should lie on a line given by a *generalized* ERE, whose coefficient, say

* zhang.10038@osu.edu

at jth order, depends on ω^2 through $\sum_{i=0} C_{i,j} b^{-4i}/M_{\rm H}^{4i}$. In the test-bed model, I used ω with near-zero values (on the order of 10^{-6} MeV, in contrast to the typical MeV scale in nuclear physics) and eigen-energies with similar size to fix $C_{i,j}$. The resulted *generalized* EREs are plotted in Fig. 1 to interpolate the extracted phase-shifts.

However, for the purpose of extracting nuclear phase shift from *ab initio* spectra calculation using Eq.(2), my previous procedure for fitting $C_{i,j}$ is not feasible, because current structure calculations adapted to computing compact nuclei would have growing and even uncontrolled errors toward small ω region. Thus, the model-independence of Eq.(2) is crucial here, because it enables an data analysis approach with controlled theoretical—series truncation—error, by treating *ab initio* results as data input. Although this is similar to extracting physics from experiments, it introduces a new approach in terms of manipulating nuclear systems using background potential that can't be realized using current engineering technology.

A by-product of deriving Eq.(2) is proving the following equality to be true in z's whole complex plane

$$\sum_{n=0}^{(R)} \frac{\Gamma\left(n+l+\frac{3}{2}\right)/\Gamma(n+1)}{z-\left(n+\frac{l}{2}+\frac{3}{4}\right)} = (-)^l \pi \frac{\Gamma\left(\frac{l}{2}+\frac{3}{4}-z\right)}{\Gamma\left(\frac{1}{4}-\frac{l}{2}-z\right)} \quad (4)$$

Both sides have the same poles and residues, but the series is divergent and needs to be properly regularized using EFT [as noted by (R)]. The rest of the paper is devoted to the derivation of Eq.(2) and the proof of Eq.(4) with a particular emphasis on *renormalization and new interaction vertices between background field and particles*. A short summary is provided in the end. To illustrate Eq.(2), two particular potential models are discussed in the supplemental materials (SM): a hard-sphere potential model is exactly solved, while the aforementioned test-bed model is numerically studied. Some details in proving Eq.(4) are also included in the SM.

Derivation through EFT— There are many possible vertices to couple background field with particle fields. However specific to harmonic potential, the CM dof is decoupled from internal dynamics and thus behaves as a free particle in its corresponding harmonic potential. This property significantly constrains forms of those vertices, which in turn are directly related to $C_{i\neq 0,j}$ terms in Eq.(2). I start with writing down a full lagrangian for l partial wave:

$$\mathscr{L}_0 = \left(c^*,\, n^*,\, \sigma_l \phi^*_{m_l}\right) \mathrm{diag}\left(i\partial_t - \hat{m}_c\psi + \frac{\boldsymbol{\partial}^2}{2M_c} + \Delta_c, i\partial_t - \hat{m}_n\psi + \frac{\boldsymbol{\partial}^2}{2M_n} + \Delta_n, i\partial_t - \hat{m}_\phi\psi + \frac{\boldsymbol{\partial}^2}{2M_{nc}} + \Delta_l\right)\left(c,\, n,\, \phi^{m_l}\right)^T,$$

$$\mathscr{L}_I = g_l \phi^*_{m_l} c \left[V^{\otimes l}\right]^{m_l} n + \mathrm{C.C} - \phi^*_{m_l}\left[d^{(l)}_{j\geq 2}\left(i\partial_t - \hat{m}_\phi\psi + \frac{\boldsymbol{\partial}^2}{2M_{nc}}\right)^j + d^{(l)}_{j\geq 0,k\geq 1}\left(i\partial_t - \hat{m}_\phi\psi + \frac{\boldsymbol{\partial}^2}{2M_{nc}}\right)^j\left(\frac{M_{\rm R}^2}{3m}\boldsymbol{\partial}^2\psi\right)^k\right]\phi^{m_l}.$$

Here c and n are the fields for two particles, while the background field $\psi(x)$ is $\frac{1}{2}m\omega^2\boldsymbol{r}^2$ with m as a reference mass. The couplings between c n ϕ and ψ are proportional to the particles' masses, i.e., $\hat{m}_c \equiv M_c/m$, $\hat{m}_n \equiv M_n/m$, and $\hat{m}_\phi \equiv M_{nc}/m$ with $M_{nc} \equiv M_n + M_c$. The short-distance interaction parts in $\mathscr{L}_0$ and the g_l coupling in $\mathscr{L}_I$ follows closely the previous works using a dimer-field approach [13, 14, 16–19]: the dimer-field ϕ^{m_l} has spin l and its projection m_l. Both l and m_l also represents the relative angular momentum and its projection of the c-n configuration that couple to ϕ; σ_l can be $+1$ or -1 but chosen to reproduce the sign for the effective range parameter[19]; in the g_l coupling, V picks up the relative velocity between n and c, while $V^{\otimes l}$ symbolically denotes a rank-l operator composed of l copies of V and is normalized such that when $m_l = +l$, $\left[V^{\otimes l}\right]^{m_l} = \left(V^{+1}\right)^l$, with $V^{+1} = (V_{+1})^\dagger$ and $V_{+1} \equiv -(V^x + iV^y)/\sqrt{2}$. The σ_l, Δ_l, g_l, and $d^{(l)}_j$ reproduce the conventional ERE (see Eq.(7) and [16, 18]). Note that the repeated indices in the lagrangians are implicitly summed up, but pay attention to the summation ranges.

In the $d^{(l)}_{j,k}$ couplings, which haven't been studied in the previous works, $M_{\rm R}^2\boldsymbol{\partial}^2\psi/(3m) = M_{\rm R}^2\omega^2 = b^{-4}$; the ∂^2 operator here is critical for making sure the dynamics of CM is a free particle in a trap except the energy is shifted by an $\boldsymbol{r}$ independent but ω^2 dependent functions: (1) terms such as ψ^2, ψ^3,,, (2) $(\boldsymbol{\partial}\psi)^4$, $(\boldsymbol{\partial}\psi)^6$,,, (note $(\boldsymbol{\partial}\psi)^2$ can be absorbed into the the $\hat{m}_\phi$ coupling in $\mathscr{L}_0$), and (3) products of (1) and (2) terms would all distort its dynamics. Even higher degree of derivatives applied on ψ would render zero contributions. It should be added that Δ_c and Δ_n could have similar couplings as Δ_l gets modified by $d^{(l)}_{j=0,k}$ couplings. Here we assume the internal scales of the particles are large enough such that the trap-induced modifications don't need to be included in the construction of Lagrangian, and the energy is measured against n-c threshold and thus $\Delta_c = \Delta_n = 0$.

It should be pointed out that ψ can be coupled to the $\phi^* nc$ operators [e.g., g_l coupling term], which again must take the form of $\left(\boldsymbol{\partial}^2\psi\right)^{1,2,,,}$. However, these terms can be eliminated by re-scaling ϕ field by a factor, $1 + \#_1 b^{-4} + ...$, while the other re-scaling-induced terms are already present in the current lagrangian (i.e., the $d^{(0)}_{j,k}$ couplings). Therefore, such trap modification to the g_l

coupling is not included here.

Based on $\mathscr{L}_{0,I}$, the one-loop self-energy bubble diagram in free space, defined through $(2\pi)^3\delta(\boldsymbol{P}-\boldsymbol{P}')\delta^{m_l}_{m_l'}\Sigma(E_{_L},\boldsymbol{P}) \equiv \langle\phi^{m_l'}_{\boldsymbol{P}'}|V_s\left(E_{_L}-H_0+i0^+\right)^{-1}V_s|\phi^{m_l}_{\boldsymbol{P}}\rangle$. H_0 is the leading order Hamiltonian, V_s is the short-distance interaction, and $\boldsymbol{P}$ and $\boldsymbol{P}'$ are momenta of CM dof, and m_l and m_l' are the spin projection of ϕ field. Σ can be computed within time-independent perturbation formalism [20] and by using two different regularization schemes: power divergence subtraction (PDS) [21] and hard momentum cut-off [12]

$$\begin{aligned}\Sigma(E) &= \frac{\mathscr{A}_l}{\pi}\int_0^{T_\Lambda} dT_q \frac{(2M_{_R}T_q)^{l+\frac{1}{2}}}{E-T_q+i0^+} \text{ cut-off}\\ &= -\mathscr{A}_l\big[ip^{2l+1}+\sum_{j=0}^{l}\frac{2\Lambda^{2j+1}}{2j+1}p^{2(l-j)}+O(\frac{1}{\Lambda})\big]\\ \Sigma(E) &= -\mathscr{A}_l(ip+2\mu)p^{2l} \text{ PDS}\\ \mathscr{A}_l &\equiv \frac{g_l^2}{M_{_R}^{2l-1}}\frac{2^{l-1}}{\pi}\frac{l!^2}{(2l+1)!}\end{aligned} \tag{5}$$

Here, $T_q \equiv \boldsymbol{q}^2/(2M_{_R})$, $p \equiv \sqrt{2M_{_R}\left(E+i0^+\right)}$, and $T_\Lambda \equiv \Lambda^2/(2M_{_R})$ with Λ as the cut off on the integration over the relative momentum $\boldsymbol{q}$. From now on $E \equiv E_{_L}-\boldsymbol{P}^2/(2M_{nc})$ is the energy in the CM frame, in contrast to $E_{_L}$ as the energy in the Lab frame.

The ϕ's full propagator in free space using the PDS scheme, defined through $(2\pi)^3\delta(\boldsymbol{P}-\boldsymbol{P}')\delta^{m_l}_{m_l'}D(E_{_L},\boldsymbol{P}) \equiv \langle\phi^{m_l'}_{\boldsymbol{P}'}|\left[E_{_L}-(H_0+V_s)+i0^+\right]^{-1}|\phi^{m_l}_{\boldsymbol{P}}\rangle$ can be computed by summing all the self-energy-insertion diagrams due to Σ and the $d_j^{(l)}$ vertices:

$$D = \frac{1}{\sigma_l(E+\Delta_l)-d_j^{(l)}E^j-\Sigma} = \frac{-\mathscr{A}_l^{-1}}{p^{2l+1}[\cot\delta_l-i]}\ , \tag{6}$$

$$\frac{p^{2l+1}}{M_{_H}^{2l+1}}\cot\delta_l = \sum_{j=0}^{\infty}C_{i=0,j}\left(\frac{p^2}{M_{_H}^2}\right)^j \text{ with } C_{0,0}=\frac{\sigma_l\Delta_l}{M_{_H}^{2l+1}\mathscr{A}_l}\ ,$$

$$C_{0,1}=\frac{\sigma_l M_{_H}^{1-2l}}{2M_{_R}\mathscr{A}_l}\ , C_{0,j\geq 2}=\frac{d_j^{(l)}M_{_H}^{2j-2l-1}}{(2M_{_R})^2\mathscr{A}_l},\ldots \tag{7}$$

The connection between D and δ_l is realized through T matrix, which is computed by multiplying D with two g_l-vertex functions [20]. Note for a given partial wave l using PDS, an -2μ should be added in defining $C_{0,j=l}$, e.g., when $l=0$, $C_{0,0}=\sigma_l\Delta_l/(M_{_H}^{2l+1}\mathscr{A}_l)-2\mu$.

Now let's turn to the trapped system. Based on $\mathscr{L}_0$, we can expand the field operators using harmonic-oscillator wave function as basis. For example, the eigenmode for c field is

$$R^{(c)}_{\boldsymbol{N}_c}(\boldsymbol{r}) = \mathscr{N}_{N_cl_c}\left(\frac{r}{b_c}\right)^{l_c}L^{l_c+\frac{1}{2}}_{N_c}\left(r^2/b_c^2\right)e^{-\frac{r^2}{2b_c^2}}Y_{l_cm_{l_c}}(\hat{r}) \tag{8}$$

Here, $\boldsymbol{N}_c \equiv (N_c,l_c,m_{l_c})$ is a quantum-number vector, corresponding to radial excitation, angular momentum and its projection; $L^\alpha_N(x)$ are the generalized Laguerre polynomials [22], $\mathscr{N}_{N_cl_c} \equiv \left[2b_c^{-3}\Gamma(N_c+1)/\Gamma\left(N_c+l_c+\frac{3}{2}\right)\right]^{\frac{1}{2}}$ [9] normalizes the norm of the wave function to be 1. The corresponding energy is $E^{(c)}_{\boldsymbol{N}_c}=(2N_c+l_c+3/2)\,\omega$. To simplify notation in the later discussion, let's redefine $R^{(c)}_{\boldsymbol{N}_c}(\boldsymbol{r}) \equiv \bar{R}^{(c)}_{N_cl_c}(r)\,r^{l_c}Y_{l_cm_{l_c}}(\hat{r})$. Note the c indices label the corresponding quantities for particle c with mass M_c.

It should be emphasized again that the g_l coupling only picks up the n-c configuration whose *total* angular momentum and its projection equal the corresponding ones in $\boldsymbol{N}_\phi$ and whose *relative* angular momentum and its projection equal the ϕ's spin and the spin projection (l and m_l). Thus the matrix element defining self-energy is $\delta^{\boldsymbol{N}_\phi'}_{\boldsymbol{N}_\phi}\delta^{m_l'}_{m_l}\Sigma_\omega(E) \equiv \langle\phi^{m_l'}_{\boldsymbol{N}_\phi'}|V_s\left(E_{_L}-H_0\right)^{-1}V_s|\phi^{m_l}_{\boldsymbol{N}_\phi}\rangle$ (note the absence of $i0+$ in the Green's function)

$$\begin{aligned}\Sigma_\omega(E) &= \frac{g_l^2}{M_{_R}^{2l}}\frac{(2l+1)!}{2^{l+2}\pi}\sum_{n=0}^{n_\Lambda}\frac{\left(\bar{R}^{(r)}_{n,l}(0)\right)^2}{E-E^{(r)}_{n,l}}\\ &= \frac{\mathscr{A}_l}{\pi}\left(\frac{2}{b}\right)^{2l+1}\sum_{n=0}^{n_\Lambda}f_l\left(z_{_E},n\right)\ .\end{aligned} \tag{9}$$

Here $f_l(z_{_E},n)$ is the *summand* in Eq.(4) with z substituted by $z_{_E}$. In the derivation, a unitary transformation between a direct product of singe particle eigenmode functions, $R^{(n)}_{\boldsymbol{N}_n}(\boldsymbol{r}_n)R^{(c)}_{\boldsymbol{N}_c}(\boldsymbol{r}_c)$, and a direct product of CM and relative motion's eigenmode functions, $R^{(cm)}_{\boldsymbol{N}_{cm}}(\boldsymbol{R})R^{(r)}_{\boldsymbol{N}_r}(\boldsymbol{r})$ has been used. $\boldsymbol{N}_r$ has n,l as the entries for radial excitation and angular momentum. Note here the relative energy $E \equiv E_{_L}-E^{(\phi)}_{\boldsymbol{N}_\phi}$ (if Δ_c and Δ_n receive trap-dependent corrections, these corrections need to be also subtracted in defining E); $z_{_E} \equiv E/(2\omega)$. (In the following, without explicit explanation, variables are for relative motion, e.g., $b=1/\sqrt{M_{_R}\omega}$.) Note here I apply a cut off on n summation to regularize the theory in a trap, which is in parallel with the cut-off regularization used in the free space calculation of the self-energy in Eq.(5). Now, I compute the ϕ's propagator in the trap, defined as $D_\omega(E)\delta^{\boldsymbol{N}_\phi'}_{\boldsymbol{N}_\phi}\delta^{m_l'}_{m_l}$, by summing up all the self-energy insertion diagrams including insertions of Σ_ω and those of the $d_j^{(l)}$ and $d^{(l)}_{j,k}$ vertices. I get

$$\begin{aligned}D_\omega &= \frac{1}{\sigma_l(E+\Delta_l)-d_j^{(l)}E^j-\Sigma_\omega(E)-d^{(l)}_{j,k}E^jb^{-4k}}\\ &= \frac{(-)\mathscr{A}_l^{-1}}{p^{2l+1}\cot\delta_l+\mathscr{A}_l^{-1}\left(\Sigma_\omega(E)-\mathscr{P}\Sigma(E)+d^{(l)}_{j,k}E^jb^{-4k}\right)}\end{aligned} \tag{10}$$

Here in the implicit summations, $d_j^{(l)}$ has $j\geq 2$ and $d^{(l)}_{jk}$ has $j\geq 0$ and $k\geq 1$. In the second step, I have added and subtracted the principle value of the free space self energy, $\mathscr{P}\Sigma$, (note the absence of $i0+$ in defining Σ_ω). Thus, the quantization condition can be derived by setting the denominator in the above equation to zero:

$$p^{2l+1}\cot\delta_l(E)+\frac{d^{(l)}_{j,k}}{\mathscr{A}_l}E^jb^{-4k} = \frac{\mathscr{P}\Sigma(E)-\Sigma_\omega(E)}{\mathscr{A}_l} \tag{11}$$

There exists a special relation between Λ and n_Λ—or a specific regularization scheme—such that the divergences in Σ and Σ_ω cancel in Eq.(11), and thus $d^{(l)}_{j,k}$ are finite. In this scheme, Eq.(11)'s RHS becomes

$$-\frac{1}{\pi}\left(\frac{2}{b}\right)^{2l+1}\left[\sum_{n=0}^{n_\Lambda} f_l\left(z_{_E},n\right)+\sum_{j=0}^{l}\frac{2z_{_E}^{l-j}}{2j+1}\left(\frac{\bar{T}_\Lambda}{2}\right)^{j+\frac{1}{2}}\right]$$
$$\equiv -\frac{1}{\pi}\left(\frac{2}{b}\right)^{2l+1}\sum_{n=0}^{(R)} f_l\left(z_{_E},n\right) \tag{12}$$

Here $\bar{T}_\Lambda \equiv T_\Lambda/\omega$. To derive this relationship, the n_Λ-dependence of Σ_ω needs to be studied. Two formulas are useful here for understanding $f_l(z_E,n)$ at large n and Σ_ω at large n_Λ. First is [23, Eq. 5.11.13]: with $z\to\infty$

$$\frac{\Gamma(z+a)}{\Gamma(z+b)}\sim\sum_{k=0}^{+\infty}\frac{G_k(a,b)}{z^{k-a+b}}\ \text{if}\ \arg(z)\le\pi-0^+ \tag{13}$$

Here a and b are real or complex constants, $G_k(a,b)$ as a function of a and b is related to the generalized Bernoulli polynomials [23, Eq. 5.11.13] [24]. The second is the Euler–Maclaurin (EM) formula [23, Eq. 2.10.1], stating for a smooth $f(x)$, its series sum can be approximated using an asymptotic expansion:

$$\sum_{n}^{n_\Lambda} f(n)\sim\int^{n_\Lambda} f(x)dx+\frac{f(n_\Lambda)}{2}+\sum_{s=1}^{+\infty}\frac{B_{2s}f^{(2s-1)}(n_\Lambda)}{(2s)!}. \tag{14}$$

Here only the n_Λ dependent terms are shown, and B_n is the Bernoulli number. As in $\Sigma(E)$, the 0th to lth E-derivatives on $\Sigma_\omega(E)$ are divergent. Thus, for s-wave we only consider $\Sigma_\omega(0)$:

$$\sum_{n}^{n_\Lambda} f_0\left(0,n\right)=\sum_{n}^{n_\Lambda}\frac{(-)}{\sqrt{n}}\left[1+O(\frac{1}{n})\right]\sim -2n_\Lambda^{\frac{1}{2}}+O(n_\Lambda^{-\frac{1}{2}}),$$

Thus $\bar{T}_\Lambda=2n_\Lambda(1+O(n_\Lambda^{-1}))$ so that the divergence can be absorbed by the $\sqrt{2\bar{T}_\Lambda}$ in Eq.(12). Notice that the $O(n_\Lambda^{-1})$ term in the derived relationship is not relevant when $n_\Lambda\to\infty$. For p-wave, the 0th and 1st E-derivatives are divergent:

$$\sum_{n}^{n_\Lambda} f_1\left(0,n\right)\sim -\frac{2}{3}n_\Lambda^{\frac{3}{2}}-\frac{7}{4}n_\Lambda^{\frac{1}{2}}+\text{const}+O\left(n_\Lambda^{-\frac{1}{2}}\right), \tag{15}$$
$$\sum_{n}^{n_\Lambda}\partial_{z_{_E}} f_1\left(z_{_E},n\right)|_{z_{_E}=0}\sim -2n_\Lambda^{\frac{1}{2}}+\text{const}+O\left(n_\Lambda^{-\frac{1}{2}}\right).$$

Thus, $\bar{T}_\Lambda/2=n_\Lambda\left(1+7/4n_\Lambda^{-1}+O(n_\Lambda^{-2})\right)$, to have all the divergences canceled by those in $\mathscr{P}\Sigma(E)$ in Eq. (12). This requires the $7/4n_\Lambda^{-1}$ piece in the expression to be specified, but even higher order terms are not needed. For d-wave, another order higher needs to be specified: $\frac{\bar{T}_\Lambda}{2}=n_\Lambda\left(1+\frac{9}{4}n_\Lambda^{-1}-\frac{37}{32}n_\Lambda^{-2}+O(n_\Lambda^{-3})\right)$. Such requirement is tied to the fact for a specific E-derivative order, there is a towers of divergences with different degrees (e.g.,Eq.(15)), while in free space, the power of Λ for a given E-derivative order is fixed due to the the dimensions of Λ and E. Of course, other schemes are allowed, as long as the divergence in the Eq.(11)'s RHS can be absorbed by the contact terms in the Eq.(11)'s LHS. Otherwise, the scheme violates the CM-decoupling property.

Finally, going back to Eq.(11), by redefining $d^{(l)}_{j,i}\equiv\mathscr{A}_l(2M_{_R})^jM_{_H}^{1+2l-4i-2j}C_{i,j}$ and using Eq.(4) and (12), the quantization condition in Eq.(11) gives the improved-BREW formula in Eqs.(2)-(3). Similar proof can be done using EFT without dimer field [12]. For any two-body contact term in Lagrangian, there exist terms baring the form of $\left(\boldsymbol{\partial}^2\psi\right)^{1,2,,,}$ multiplying that contact term (again the decoupling of CM from internal dynamics needs to be preserved). Since the two-body contact interactions reproduce the ERE, the trap-induced corrections modify this ERE as we already derived above.

Proof of Eq.(4)— First, I define $\tilde{f}_l(\tilde{z},n)\equiv f_l(z,n)$ with $\tilde{z}\equiv z-l/2-3/4$ and $g_l(\tilde{z})\equiv(-)^l\pi\Gamma(-\tilde{z})/\Gamma(-l-1/2-\tilde{z})$. In the proof, integrating $g_l(\tilde{u})/(\tilde{u}-\tilde{z})$ in the $\tilde{u}$'s complex plane over a large circle C around center with radius $n_\Lambda<R<n_\Lambda+1$ (thus $|\tilde{z}|\ll R$) is essential and gives

$$g_l(\tilde{z})=\sum_{n=0}^{n_\Lambda}\tilde{f}_l(\tilde{z},n)+\frac{1}{2\pi i}\oint_C d\tilde{u}\frac{g_l(\tilde{u})}{\tilde{u}-\tilde{z}}\ . \tag{16}$$

The LHS come from the residue of the $1/(\tilde{u}-\tilde{z})$ pole while the series summation in the RHS is from the residues of $g_l(\tilde{u})$'s poles on the positive real axis (note the LHS and the series sum on the RHS with $n_\Lambda\to\infty$ have the same pole structure). Comparing Eq.(16) to Eq.(4) indicates the contour integration in the Eq.(16)'s RHS should play the same role of canceling the series's divergence as $-\mathscr{P}\Sigma(E)$ in Eq.(12). By carefully reducing R to be infinitely close to n_Λ but not crossing the $\tilde{u}=n_\Lambda$ singularity and analyzing $g_l(\tilde{u})$'s behavior in two different regions: $|\arg(\tilde{u})|\gg R^{-1}$ and $|\arg(\tilde{u})|\sim R^{-1}$, it could be shown that the 2nd term in the RHS of Eq.(16) is

$$-\int_0^{n_\Lambda}\tilde{f}_l^{\text{ET}}(\tilde{z},\tilde{u})d\tilde{u}-\frac{\tilde{f}_l^{\text{E}}(\tilde{z},n_\Lambda)}{2}-\sum_{j=1}^{+\infty}\frac{B_{2j}}{(2j)!}\frac{\partial\tilde{f}_l^{\text{E}}(\tilde{z},n_\Lambda)}{\partial n_\Lambda^{2j-1}}, \tag{17}$$

with error behaves as $e^{-n_\Lambda\#}$ with $\#$ as positive constant. Here, $\tilde{f}_l^{\text{E}}(\tilde{z},\tilde{u})$ is the asymptotic expansion of $\tilde{f}_l(\tilde{z},\tilde{u})$ in terms of $1/\tilde{u}$ using Eq.(13); $\tilde{f}_l^{\text{ET}}(\tilde{z},\tilde{u})$ truncates the expansion by keeping terms with powers of $\tilde{u}$ from $l-1/2$ to $-1/2$; and the last term involves $2j-1$ derivatives wrt n_Λ. This expression coincides with the derivation of the series summation's divergence using Eq.(14), and thus concludes the proof. Further details for deriving Eq.(17) can be found in the SM.

Summary—I have applied pionless EFT to study two short-range interacting particles trapped by an external harmonic potential. It produces a systematically improved BERW formula that are exact not only in the region of near-zero ω, but also at larger ω values, as long

as both the length scale of trap b and the dynamical scale p^{-1} are larger than the range of the short-distance interaction. This provides a firm foundation for implementing a Luscher-formula-like approach in connecting nuclear scattering and current *ab initio* structure calculations. Through the derivation, a new sets of coupling terms between external field and particles have been studied, which are the source of improving the original BERW formula. Moreover, a careful analysis of renormalization shows the non-triviality in matching EFT in free space and EFT with trap turned on (i.e., the connection between cut off Λ on relative momentum and n_Λ on the number of radial excitation). The renormalization procedure is further justified by the proof of Eq.(4). Both components haven't been uncovered in the previous studies, and could provide lessons for further generalizing the improved BERW formula to studying nuclear reaction and system larger than two sub-clusters.

Acknowledgment–

[1] T. Busch, B.-G. Englert, K. Rzażewski, and M. Wilkens, Foundations of Physics **28**, 549 (1998).

[2] D. Blume and C. H. Greene, Phys. Rev. A **65**, 043613 (2002).

[3] M. Block and M. Holthaus, Phys. Rev. A **65**, 052102 (2002).

[4] E. L. Bolda, E. Tiesinga, and P. S. Julienne, Phys. Rev. A **66**, 013403 (2002).

[5] A. Suzuki, Y. Liang, and R. K. Bhaduri, Phys. Rev. A **80**, 033601 (2009).

[6] T. Luu, M. J. Savage, A. Schwenk, and J. P. Vary, Phys. Rev. C **82**, 034003 (2010), arXiv:1006.0427 [nucl-th].

[7] M. Luscher, Nucl. Phys. **B354**, 531 (1991).

[8] I. Stetcu, B. R. Barrett, U. van Kolck, and J. P. Vary, Phys. Rev. **A76**, 063613 (2007), arXiv:0705.4335 [cond-mat.other].

[9] I. Stetcu, J. Rotureau, B. R. Barrett, and U. van Kolck, Annals Phys. **325**, 1644 (2010), arXiv:1001.5071 [cond-mat.quant-gas].

[10] J. Rotureau, I. Stetcu, B. R. Barrett, and U. van Kolck, Phys. Rev. **C85**, 034003 (2012), arXiv:1112.0267 [nucl-th].

[11] S. Ali, A. A. Z. Ahmad, and N. Ferdous, Rev. Mod. Phys. **57**, 923 (1985).

[12] U. van Kolck, Nucl. Phys. **A 645**, 273 (1999), arXiv:nucl-th/9808007 [nucl-th].

[13] P. F. Bedaque and U. van Kolck, Ann. Rev. Nucl. Part. Sci. **52**, 339 (2002), arXiv:nucl-th/0203055 [nucl-th].

[14] H. W. Hammer, C. Ji, and D. R. Phillips, J. Phys. **G44**, 103002 (2017), arXiv:1702.08605 [nucl-th].

[15] S. R. Beane, P. F. Bedaque, A. Parreno, and M. J. Savage, Phys. Lett. **B585**, 106 (2004), arXiv:hep-lat/0312004 [hep-lat].

[16] R. A. Briceno, Z. Davoudi, and T. C. Luu, Phys. Rev. **D88**, 034502 (2013), arXiv:1305.4903 [hep-lat].

[17] P. F. Bedaque, H. W. Hammer, and U. van Kolck, Phys. Lett. **B 569**, 159 (2003), arXiv:nucl-th/0304007 [nucl-th].

[18] S. R. Beane and M. J. Savage, Nucl.Phys. **A694**, 511 (2001), arXiv:nucl-th/0011067 [nucl-th].

[19] D. B. Kaplan, M. J. Savage, and M. B. Wise, Phys.Lett. **B424**, 390 (1998), arXiv:nucl-th/9801034 [nucl-th].

[20] X. Zhang, K. M. Nollett, and D. R. Phillips, Phys. Rev. C **98**, 034616 (2018), arXiv:1708.04017 [nucl-th].

[21] D. B. Kaplan, M. J. Savage, and M. B. Wise, Nucl.Phys. **B534**, 329 (1998), arXiv:nucl-th/9802075 [nucl-th].

[22] M. Abramowitz and I. Stegun, *Handbook of Mathematical Functions* (Dover Publications, New York, 1972).

[23] DLMF, "*NIST Digital Library of Mathematical Functions*," http://dlmf.nist.gov/, Release 1.0.22 of 2019-03-15, f. W. J. Olver, A. B. Olde Daalhuis, D. W. Lozier, B. I. Schneider, R. F. Boisvert, C. W. Clark, B. R. Miller and B. V. Saunders, eds.

[24] N. M. Temme, *Special Functions: An Introduction to the Classical Functions of Mathematical Physics* (Wiley, 1996).

[25] C. J. Joachain, *Quantum Collision Theory* (North-Holland, Amsterdam, 1975).

[26] M. Petkovšek, H. S. Wilf, and D.Zeilberger, $A=B$ (A K Peters, Wellesley, MA, 1996) page 38.

[27] R. Furnstahl, D. Phillips, and S. Wesolowski, J.Phys. **G42**, 034028 (2015), arXiv:1407.0657 [nucl-th].

I. SUPPLEMENTAL MATERIAL

A. An exactly solvable case: hard-sphere potential

As demonstrated here, if the interaction is short-ranged and has the form of a hard sphere, the problem can be analytically solved. The model was studied in Ref. [3] by using parabolic cylinder functions for s-wave channel. Let's define the hard-sphere potential as $V_s(r) = +\infty$ if $r \leq r_c$ and 0 otherwise ($r \equiv |\boldsymbol{r}|$ with $\boldsymbol{r}$ the relative displacement between the two particles). In addition, each particle experiences an external harmonic potential. Since the CM motion is factorized, I only focus on the relative motion and the corresponding external potential is $M_{\rm R}\omega^2\boldsymbol{r}^2/2$, with $M_{\rm R}$ again as effective mass. I first rescale $\bar{r} \equiv r/b$ and $\bar{r}_c \equiv r_c/b$ with $b \equiv 1/\sqrt{M_{\rm R}\omega}$, and $\bar{E} \equiv E/\omega$. When $\bar{r} > \bar{r}_c$, the Schrodinger equation can be rewritten as

$$\left[-\frac{d^2}{d\bar{r}^2} + \frac{l(l+1)}{\bar{r}^2} + \bar{r}^2\right] u_l = 2\bar{E}u_l \ , \tag{18}$$

with the radial wave function defined as $u_l(\bar{r})/r$. Thus, the wave function at $\bar{r} > \bar{r}_c$ is a linear combination of two independent solutions to the above harmonic oscillator Schrodinger equation [5]:

$$\begin{aligned} u_l = e^{-\frac{\bar{r}^2}{2}}\Bigg[&c_1\bar{r}^{l+1}M\left(\frac{l}{2}+\frac{3}{4}-\frac{\bar{E}}{2}, l+\frac{3}{2}, \bar{r}^2\right) \\ &+c_2\bar{r}^{-l}M\left(-\frac{l}{2}+\frac{1}{4}-\frac{\bar{E}}{2}, -l+\frac{1}{2}, \bar{r}^2\right)\Bigg] \ . \end{aligned} \tag{19}$$

Here, $M(a,b,z)$ is the Kummer function [22]. When $\bar{r} \to +\infty$, u_l should approach to zero to guarantee that the wave function is normalizable. Since at large z [23, Eq. 13.7.2]

$$M\left(a,b;z\right) \approx \Gamma(b)\left[\frac{z^{a-b}e^z}{\Gamma(a)} + \frac{(-z)^{-a}}{\Gamma(b-a)}\right]\left[1+O(z^{-1})\right] \tag{20}$$

thus I get

$$c_1\frac{\Gamma\left(l+\frac{3}{2}\right)}{\Gamma\left(\frac{l}{2}+\frac{3}{4}-\frac{\bar{E}}{2}\right)} + c_2\frac{\Gamma\left(-l+\frac{1}{2}\right)}{\Gamma\left(-\frac{l}{2}+\frac{1}{4}-\frac{\bar{E}}{2}\right)} = 0 \ . \tag{21}$$

Meanwhile, $u_l\left(\bar{r}_c\right) = 0$ indicates

$$\begin{aligned} &c_1\bar{r}_c^{l+1}M\left(\frac{l}{2}+\frac{3}{4}-\frac{\bar{E}}{2}, l+\frac{3}{2}, \bar{r}_c^2\right) \\ &\quad+\frac{c_2}{\bar{r}_c^l}M\left(-\frac{l}{2}+\frac{1}{4}-\frac{\bar{E}}{2}, -l+\frac{1}{2}, \bar{r}_c^2\right) = 0 \ . \end{aligned} \tag{22}$$

Eqs.(21)-(22) would have nontrivial solutions only when the determinant is zero, which gives the quantization condition:

$$\frac{(2\bar{r}_c)^{2l+1}}{(-)^l\mathscr{N}_l}\frac{\Gamma\left(\frac{l}{2}+\frac{3}{4}-\frac{\bar{E}}{2}\right)}{\Gamma\left(\frac{1}{4}-\frac{l}{2}-\frac{\bar{E}}{2}\right)} = \frac{M\left(\frac{1}{4}-\frac{l}{2}-\frac{\bar{E}}{2}, \frac{1}{2}-l, \bar{r}_c^2\right)}{M\left(\frac{l}{2}+\frac{3}{4}-\frac{\bar{E}}{2}, l+\frac{3}{2}, \bar{r}_c^2\right)} \tag{23}$$

Here, $\mathscr{N}_l \equiv (2l+1)!!(2l-1)!!$ [note $(-1)!! \equiv 1$]. Note that the Eq.(23)'s LHS is Eq.(1)'s RHS multiplied by a $(-)r_c^{2l+1}/\mathscr{N}_l$ factor. Meanwhile, the phase shift due to $V_s(r)$ in the l partial wave is $\tan\delta_l = j_l(pr_c)/y_l(pr_c)$ [25]. Thus the deficiency of Eq.(1) could be exposed by the difference between Eq.(23)'s RHS and Eq.(1)'s LHS multiplied by $-r_c^{2l+1}/\mathscr{N}_l$, i.e.,

$$\frac{(pr_c)^{2l+1}}{(-)\mathscr{N}_l}\frac{y_l(pr_c)}{j_l pr_c)} \text{ vs. } \frac{M\left(\frac{1}{4}-\frac{l}{2}-\frac{\bar{E}}{2}, \frac{1}{2}-l, \bar{r}_c^2\right)}{M\left(\frac{l}{2}+\frac{3}{4}-\frac{\bar{E}}{2}, l+\frac{3}{2}, \bar{r}_c^2\right)} \ . \tag{24}$$

The LHS can be expanded in terms of $(pr_c)^2$:

$$1 + \frac{(2l+1)\left(pr_c\right)^2}{4l(l+1)-3} + \frac{(l+3)(2l+1)\left(pr_c\right)^4}{(2l-3)(2l+3)^2(2l+5)} + \ldots \tag{25}$$

Now according to [23, Eq.(13.2.2)], $M(a,b,z)$ can be expanded as $1 + \frac{a}{b}z + \frac{a(a+1)}{b(b+1)}\frac{z^2}{2!} + \ldots$, indicating that Eq.(24)'s RHS, a function of E and r_c, can be approximated by a double expansion in terms of powers of $\bar{r}_c^2$ and $2\bar{E}\bar{r}_c^2 = (pr_c)^2$ (note in Eq.(24) the "b"s for M function are independent of $\bar{E}$), when both are small. This also suggests the difference between LHS and RHS can also be expanded in terms of $\bar{r}_c^2$ and $2\bar{E}\bar{r}_c^2$. Now, it can be shown that with $\omega \to 0$ and E and r_c fixed, the Eq.(24)'s RHS approaches its LHS. In this limit, $\bar{E} \to \infty$, and

$$\begin{aligned} &\lim_{\omega\to 0} M\left(-\frac{l}{2}+\frac{1}{4}-\frac{\bar{E}}{2}, -l+\frac{1}{2}, \bar{r}_c^2\right) \\ &= \lim_{\omega\to 0} M\left(-\frac{E}{2\omega}, -l+\frac{1}{2}, r_c^2 M_{\rm R}\omega\right) \\ &= {}_0F_1\left(;-l+\frac{1}{2};-\frac{1}{2}M_{\rm R}Er_c^2\right) \ , \end{aligned} \tag{26}$$

$$\begin{aligned} &\lim_{\omega\to 0} M\left(\frac{l}{2}+\frac{3}{4}-\frac{\bar{E}}{2}, l+\frac{3}{2}; \bar{r}_c^2\right) \\ &= {}_0F_1\left(;l+\frac{3}{2};-\frac{1}{2}M_{\rm R}Er_c^2\right) \ , \end{aligned} \tag{27}$$

Here, ${}_0F_1$ known as Confluent Hypergeometric Limit Function. From Ref. [26],

$$J_\alpha(z) = \frac{\left(\frac{z}{2}\right)^\alpha}{\Gamma\left(\alpha+1\right)}{}_0F_1\left(;\alpha+1;-\frac{z^2}{4}\right) \ . \tag{28}$$

And since,

$$j_l(z) = \sqrt{\frac{\pi}{2z}}J_{l+\frac{1}{2}}(z) \, , y_l(z) = (-)^{l+1}\sqrt{\frac{\pi}{2z}}J_{-l-\frac{1}{2}}(z) \tag{29}$$

I get

$$\frac{{}_0F_1\left(;-l+\frac{1}{2};-\frac{1}{2}M_{\rm R}Er_c^2\right)}{{}_0F_1\left(;l+\frac{3}{2};-\frac{1}{2}M_{\rm R}Er_c^2\right)} = \frac{(pr_c)^{2l+1}}{(-)\mathscr{N}_l}\frac{y_l(pr_c)}{j_l pr_c)} \ , \tag{30}$$

and thus proves the difference between the two sides of Eq.(24) disappears at $\omega \to 0$. This requires that the difference if expanded in terms of $\bar{r}_c^2$ and $2\bar{E}\bar{r}_c^2$, must have positive powers of $\bar{r}_c^2$ (note $\propto \omega$).

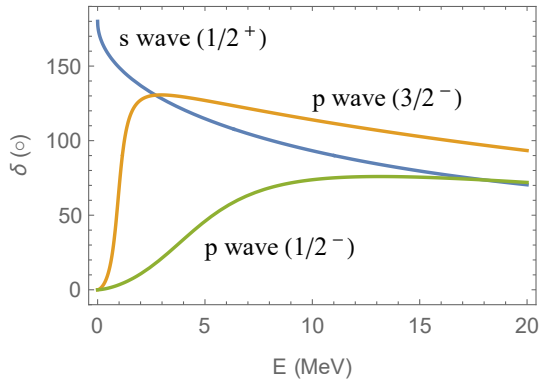

FIG. 2. The neutron-α scattering phase shifts in s and p waves vs. their CM energy E, as produced by the model potential well [11].

Moreover Eq.(24)'s RHS is unchanged with $\bar{E} \to -\bar{E}$ and $\bar{r}_c^2 \to -\bar{r}_c^2$ (i.e., $\omega \to -\omega$), because $M(a,b,z) = e^z\, M(b-a,b,-z)$[23, Eq.(13.2.39)], indicating that the powers of $\bar{r}_c^2$ are even. Therefore, the following expansion is expected with the first two terms explicitly derived:

$$\begin{aligned}
&\frac{(-1)^{l+1}}{\mathscr{N}_l}\left(\frac{2r_c}{b}\right)^{2l+1}\frac{\Gamma\left(\frac{3}{4}+\frac{l}{2}-\frac{\bar{E}}{2}\right)}{\Gamma\left(\frac{1}{4}-\frac{l}{2}-\frac{\bar{E}}{2}\right)}-\frac{(pr_c)^{2l+1}\cot\delta_l(p)}{\mathscr{N}_l}\\
=&\frac{(2l+1)\left(\frac{r_c}{b}\right)^4}{2(2l-3)(2l+5)}+\frac{(2l+1)(6l+25)(pr_c)^2\left(\frac{r_c}{b}\right)^4}{6(2l-5)(2l+3)(2l+5)(2l+7)}+\ldots\\
\equiv&\sum_{i=1}^{\infty}\sum_{j=0}^{\infty}C_{i,j}\left(\frac{r_c}{b}\right)^{4i}(pr_c)^{2j} \qquad (31)
\end{aligned}$$

Meanwhile the ERE for V_s can be derived easily from Eq.(25): $(pr_c)^{2l+1}\cot\delta_l(p)/\mathscr{N}_l = \sum_{j=0}^{\infty} C_{i=0,j}\,(pr_c)^{2j}$. If the reference scale $M_{_H} = r_c^{-1}$ is identified, we get the the formula similar to Eqs.(2)-(3), except the extra overall normalization $\mathscr{N}_l^{-1}$. This normalization can but is not absorbed into the definition of $M_{_H}$ in order to guarantee series convergence for large l.

B. The 2nd model for numerical testing

Here I use a simple square potential well model [11] to test the proposed improved BREW formula. The potential was constructed to qualitatively describes neutron-α nucleus scatterings in s- and p-waves [11]. The quantum numbers for the studied channels in terms J^π notation are $\frac{1}{2}^+$, $\frac{1}{2}^-$ and $\frac{3}{2}^-$. The potential $V_s(r) = V_0(1+\beta \boldsymbol{L}\cdot\boldsymbol{\sigma})$ when $r < r_c$ and 0 when $r > r_c$, with $V_0 = -33$ MeV, $r_c = 2.55$ fm, $\beta = 0.103$ [11]. $\boldsymbol{L}\cdot\boldsymbol{\sigma}$ is the spin-orbital coupling, providing difference between $p_{\frac{3}{2}}$ and $p_{\frac{1}{2}}$ channels. Here, this interaction is treated as the exact underlying physics for two particles. The corresponding phase shifts, as calculated by solving the corresponding schrodinger equation in the continuum, are shown in Fig. 2. These phase shifts are considered as "exact" phase shift. Meanwhile, the spectra for the two particles in various harmonic potential wells can also be precisely computed. My goal is to test the original and the improved BERW formula using these exact phase-shifts and energy spectra.

	$i=1$	2	3
$j=0$	-0.4097	0.004206	0.2334
1	-0.1756	-0.4063	0.5012
2	0.2010	-0.5742	
3	0.2949	-0.2036	
4	0.1491	-0.1586	
5	-0.01443		
6	-0.07766		

TABLE I. $C_{i\geq 1,j}$ for the $s_{1/2}$ channel.

	$i=1$	2	3
$j=0$	-1.870	0.5400	-0.08928
1	-0.8676	0.3118	0.1352
2	-0.2829	-0.009065	
3	-0.03911	-0.09838	
4	0.01474	-0.05651	
5	0.01222		
6	0.004617		

TABLE II. $C_{i\geq 1,j}$ for the $p_{3/2}$ channel.

	$i=1$	2	3
$j=0$	-2.084	0.7400	-0.2041
1	-1.090	0.5210	0.03088
2	-0.4064	0.1012	
3	-0.08700	-0.06392	
4	0.001002	-0.05106	
5	0.009643		
6	0.004640		

TABLE III. $C_{i\geq 1,j}$ for the $p_{1/2}$ channel.

In Fig. 3, the difference between the two sides in Eq.(1) divided by $M_{_H}^{2l+1}$ at eigen-energies corresponding to a set of trap frequencies ($\omega = 0.1$, $\sqrt{0.1}$, 1, $\sqrt{10}$ and 10 MeV) are plotted. Here I set $M_{_H} = 1\text{fm}^{-1}$, as motivated by the value of r_c. The immediate observation is that the leading order different does scale as ω^2. In the s-wave channel, there exists a deep bound state in free space—not physical for neutron-α system—and thus a distinct negative eigen-energy in all the chosen traps. However for other two channels, no bound state exists in free space. To see how well the improved BERW formula works, I have computed a set of exact phase shifts and

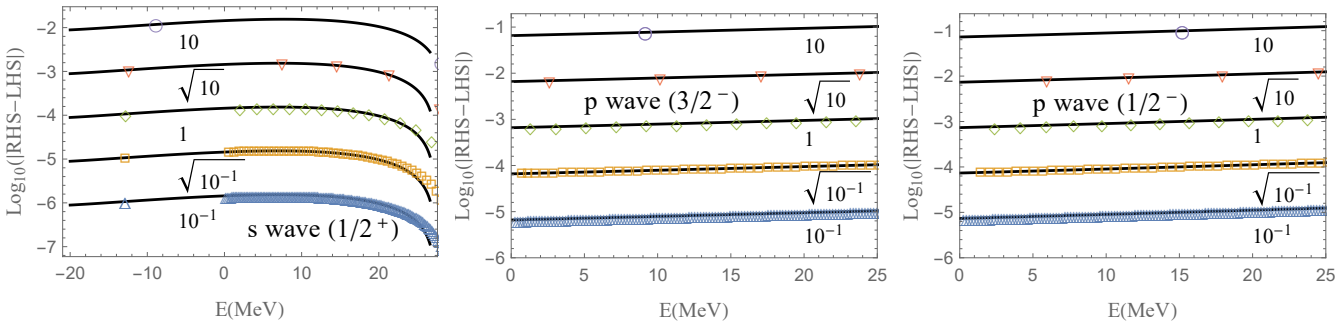

FIG. 3. The y axis is $\log_{10}\left(|\mathrm{LHS}-\mathrm{RHS}|/M_H^{2l+1}\right)$ in the original BERW formula (Eq.(1)) with $M_H = 1\mathrm{fm}^{-1}$, while the x axis is the energy. Three different channels are plotted in different panels. The symbols are the differences computed at those exact eigen-energies corresponding to various harmonic potential traps with six ω values: 0.1, $\sqrt{0.1}$, 1, $\sqrt{10}$ and 10 MeV. Meanwhile the curves are the trap-dependent corrections in the improved-BERW formula with $C_{i\neq 0,j}$ parameters fitted as described in the text.

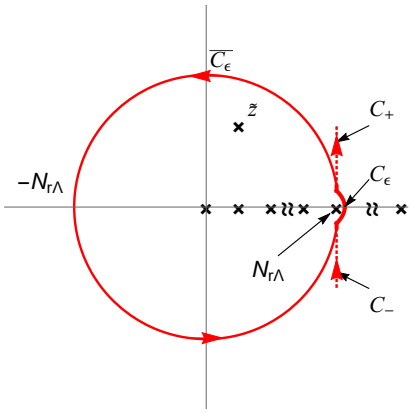

FIG. 4. The contours for the integration in $\tilde{u}$'s complex plane. C_ϵ is a small circle around the pole at $\tilde{u} = n_\Lambda$ with radius ϵ, which intersects with a large circle around the center with radius $R = n_\Lambda$. The $C_\pm$ originates from the intersections and goes $\pm i\infty$ in parallel to the imaginary axis.

eigen-energies (on the order of 10^{-6} MeV) at extremely small trap frequencies (on the order of 10^{-6} MeV), used the $C_{i,j}$ terms in the improved BERW formula to fit the differences in the region with $E \sim 10^{-6}$ MeV. The resulted fits are plotted in Fig. 3 to interpolate the RHS and LHS difference computed at discreete eigen-energies up to much larger energy region (up to 20 MeV). The corresponding parameters are shown in Tables I, II, and III. A few higher-order $C_{i,j}$ values are not shown in table, because the over-fitting [27] in this simple exercise gives values with size significantly larger than 1 (however their contributions are very small in the shown plots, and set to be zero). It can be concluded that the deficiency of Eq.(1) can indeed be expanded in terms of powers of b^{-4} and E as indicated by the improved BERW formula.

C. Details in proving Eq.(4)

As mentioned in the main text, $\tilde{f}_l(\tilde{z},n) \equiv f_l(z,n)$ with $\tilde{z} \equiv z - l/2 - 3/4$ and $g_l(\tilde{z}) \equiv (-)^l\pi\Gamma(-\tilde{z})/\Gamma(-l-1/2-\tilde{z})$. Eq.(4) now becomes

$$\sum_{n=0}^{(R)} \tilde{f}_l(\tilde{z},n) = g_l(\tilde{z})\ . \tag{32}$$

To proceed, I deform the contour C (a circle with R around center and $n_\Lambda < R < n_\Lambda + 1$) as mentioned in Eq.(16) to $\overline{C_\epsilon} + C_\epsilon$ as plotted in Fig. 4 by reducing R to n_Λ but still enclosing the $\tilde{u} = n_\Lambda$ singularity. Eq.(16) now becomes

$$g_l(\tilde{z}) = \sum_{n=0}^{n_\Lambda} \tilde{f}_l(\tilde{z},n) + \frac{1}{2\pi i}\oint_{\overline{C_\epsilon}+C_\epsilon} d\tilde{u}\frac{g_l(\tilde{u})}{\tilde{u}-\tilde{z}} \tag{33}$$

As argued in the main text, the contour integration in Eq.(33) (or Eq.(16)) should cancel the series's divergence as $-\mathscr{P}\Sigma(E)$ in Eq.(12) does. This is the focus on the following proof. First, It is important to understand the behavior of $g_l(\tilde{u})$ in two different regions: $|\arg(\tilde{u})| \gg R^{-1}$ and $|\arg(\tilde{u})| \sim R^{-1}$. Using [23, Eq. 5.5.3] I re-express

$$g_l(\tilde{u}) = \pi\cot(\pi\tilde{u})\frac{\Gamma\left(l+\frac{3}{2}+\tilde{u}\right)}{\Gamma(1+\tilde{u})}\ . \tag{34}$$

Then, with $R \to +\infty$,

$$\cot(\pi\tilde{u}) = i\frac{e^{i\pi\tilde{u}}+e^{-i\pi\tilde{u}}}{e^{i\pi\tilde{u}}-e^{-i\pi\tilde{u}}} = \begin{cases}(-i)\,\text{if}\,\arg(\tilde{u}) \gg R^{-1}\\ (+i)\,\text{if}\,\arg(\tilde{u}) \ll -R^{-1}\end{cases} \tag{35}$$

Therefore, $\cot(\pi\tilde{u}) \sim -i\,\mathrm{sgn}(\mathrm{Im}\tilde{u})$ when $|\arg(\tilde{u})| \gg R^{-1}$ (the error scales as $e^{-R\#}$ with $\#$ as a positive number), which behaves like a branch cut on the positive real axis. However $\cot(\pi\tilde{u})$ has only poles on that axis, indicating its behavior at $|\arg(\tilde{u})| \sim R^{-1}$ is qualitatively different. Also note that the Γ function ratio in Eq.(34) is the same

as that ratio in $\tilde{f}_l(\tilde{z},n)$ with $n\to\tilde{u}$. Applying the asymptotic expansion from Eq.(13) on the Eq.(34)'s RHS, I get when $R\gg|\tilde{z}|$

$$\frac{g_l(\tilde{u})}{\tilde{u}-\tilde{z}}\sim -i\,\mathrm{sgn}(\mathrm{Im}\tilde{u})\pi\left(\sum_{k=0}^{+\infty}\frac{G_k(l+\frac{3}{2},1)}{\tilde{u}^{k-l-\frac{1}{2}}}\right)\sum_{k'=0}^{+\infty}\frac{\tilde{z}^{k'}}{\tilde{u}^{k'+1}} \tag{36}$$

The above expression is the same as $i\,\mathrm{sgn}(\mathrm{Im}\tilde{u})\pi\tilde{f}_l^{\mathrm{E}}(\tilde{z},\tilde{u})$, while $\tilde{f}_l^{\mathrm{E}}(\tilde{z}.\tilde{u})$, as mentioned in the main text, is the asymptotic expansion of $\tilde{f}_l(\tilde{z},\tilde{u})$ using Eq.(13). Thus, I split the contour integration to two major pieces,

$$\oint_{\overline{C_\epsilon}+C_\epsilon} d\tilde{u}\,\{i\,\mathrm{sgn}(\mathrm{Im}\tilde{u})-[\cot(\pi\tilde{u})+i\,\mathrm{sgn}(\mathrm{Im}\tilde{u})]\}\,\frac{\tilde{f}_l^{\mathrm{E}}(\tilde{z},\tilde{u})}{2i} \tag{37}$$

Integrating the first piece from over $\overline{C_\epsilon}$ with $\epsilon\to 0^+$ gives

$$\begin{aligned}&\int_{0^+\le\theta_{\tilde{u}}<2\pi} d\tilde{u}\,\frac{\tilde{f}_l^{\mathrm{E,T}}(\tilde{z},\tilde{u})}{2}=\int_{0^+\le\theta_v<\pi} dv\,v\tilde{f}_l^{\mathrm{E,T}}(\tilde{z},v^2)\\&=\int_{-\sqrt{R}}^{\sqrt{R}}dv(-)v\tilde{f}_l^{\mathrm{E,T}}(\tilde{z},v^2)=(-)\int_0^R d\tilde{u}\tilde{f}_l^{\mathrm{E,T}}(\tilde{z},\tilde{u})\end{aligned} \tag{38}$$

As also defined in the main text, $\tilde{f}_l^{\mathrm{E,T}}(\tilde{z},\tilde{u})$ only keeps terms with powers of $\tilde{u}$ no smaller than $-1/2$ from $\tilde{f}_l^{\mathrm{E}}(\tilde{z},\tilde{u})$, because the neglected terms' integration vanishes no slower than $O(1/\sqrt{R})$ as $R\to\infty$. In the derivation, I have (1) rotated the $-\pi\le\arg(\tilde{u})\le 0^+$ branch by $+2\pi$ angle and eliminated $\mathrm{sgn}(\mathrm{Im}\tilde{u})$ because the integrand has $\sqrt{\tilde{u}}$ factor,(2) used $\tilde{u}=v^2$ transformation and (3) that $v\tilde{f}_l^{\mathrm{E,T}}(\tilde{z}v^2)$ is analytical in v's upper complex plane and even function on the real axis. Note integrating the first piece over C_ϵ gives 0 when $\epsilon\to 0^+$. For the 2nd major piece, its contour contribution $\overline{C_\epsilon}+C_\epsilon$ can be approximated by $C_+ + C_- + C_\epsilon$, with $C_\pm$ noted in Fig. 4 and error scaling as $e^{-R\#}$ with $\#$ as positive constant. Since $\cot(\pi\tilde{u})\sim 1/[\pi(\tilde{u}-n_\Lambda)]$ with $\tilde{u}\to n_\Lambda$, the C_ϵ contour contribution with $\epsilon\to 0^+$ gives $(-)\tilde{f}_l^{\mathrm{E}}(\tilde{z},n_\Lambda)/2$. While the $C_+ + C_-$ contour integration gives (with $\epsilon\to 0^+$)

$$\begin{aligned}&\int_{C_++C_-} d\tilde{u}\,[\cot(\pi\tilde{u})+i\,\mathrm{sgn}(\mathrm{Im}\tilde{u})]\,(-)\frac{\tilde{f}^{\mathrm{E}}(\tilde{z},\tilde{u})}{2i}\\&=\int_\epsilon^{+\infty} i\,d\Delta\frac{\tilde{f}^{\mathrm{E}}(\tilde{z},n_\Lambda+i\Delta)}{e^{2\pi\Delta}-1}-\int_{-\infty}^{-\epsilon} i\,d\Delta\frac{\tilde{f}^{\mathrm{E}}(\tilde{z},n_\Lambda+i\Delta)}{e^{-2\pi\Delta}-1}\\&=\int_0^{+\infty}\frac{d2\pi\Delta}{2\pi i}\frac{\left[\tilde{f}_l^{\mathrm{E}}(\tilde{z},n_\Lambda-i\Delta)-\tilde{f}_l^{\mathrm{E}}(\tilde{z},n_\Lambda+i\Delta)\right]}{e^{2\pi\Delta}-1}\\&\sim(-)\sum_{j=1}^{+\infty}\tilde{f}_l^{\mathrm{E},(2j-1)}(\tilde{z},n_\Lambda)\frac{B_{2j}}{(2j)!}\end{aligned} \tag{39}$$

Because the integration is dominated by the $\Delta\ll n_\Lambda$ region, the two $\tilde{f}_l^{\mathrm{E}}$ are expanded in terms of Taylor series for the 2nd argument at n_Λ. The resulted integrations are proportional to Riemann $\zeta(2j)$ at even arguments, which are related to Bernoulli numbers [23, Eq. 25.5.1, 25.6.2, 24.2.2]. Adding all the contributions, we have the 2nd term in the RHS of Eq.(16) is given in Eq.(17), with error behaves as $e^{-n_\Lambda\#}$ with $\#$ as positive constant. The above expression coincides with the derivation of the series summation's divergence using Eq.(14), and thus concludes the proof.